Commun. Comput. Phys.
doi: 10.4208/cicp.100614.270315a

Vol. **18**, No. 5, pp. 1461-1481
November 2015

Efficient Operator Marching Method for Analyzing Crossed Arrays of Cylinders

Yu Mao Wu[1] and Ya Yan Lu[2,*]

[1] *Key Laboratory for Information Science of Electromagnetic Waves (MoE), School of Information Science and Technology, Fudan University, Shanghai, China.*
[2] *Department of Mathematics, City University of Hong Kong, Kowloon, Hong Kong.*

Received 10 June 2014; Accepted (in revised version) 27 March 2015

Abstract. Periodic structures involving crossed arrays of cylinders appear as special three-dimensional photonic crystals and cross-stacked gratings. Such a structure consists of a number of layers where each layer is periodic in one spatial direction and invariant in another direction. They are relatively simple to fabricate and have found valuable applications. For analyzing scattering properties of such structures, general computational electromagnetics methods can certainly be used, but special methods that take advantage of the geometric features are often much more efficient. In this paper, an efficient method based on operators mapping electromagnetic field components between two spatial directions is developed to analyze structures with crossed arrays of circular cylinders. The method is much simpler than an earlier method based on similar ideas, and it does not require evaluating slowly converging lattice sums.

AMS subject classifications: 78M25, 78M16, 78A45

Key words: Periodic structure, Photonic crystal, Operator marching, Scattering problem.

1 Introduction

Periodic structures such as diffraction gratings [1–3], photonic crystals [4] and metamaterials [5], have many interesting and useful properties, and are very important in modern photonics technologies. In this paper, we consider three-dimensional (3D) biperiodic structures consisting of crossed arrays of cylinders. More precisely, we assume the structures are periodic in the x and y directions, and bounded by homogeneous media in the z direction, where $\{x,y,z\}$ is a Cartesian coordinate system. In the z direction, it is further assumed that the structure can be divided into a number of layers, where each layer

*Corresponding author. *Email addresses:* yumaowu@fudan.edu.cn (Y. M. Wu), mayylu@cityu.edu.hk (Y. Y. Lu)

is a periodic array of cylinders parallel to the x or y axis. Such crossed arrays of cylinders are relatively easy to fabricate, and appear as special 3D photonic crystals [6,7] and cross-stacked gratings [8].

For biperiodic structures bounded by homogeneous media in the z direction, a fundamental problem is to compute the transmitted and reflected waves for a given plane incident wave [9–12]. For electromagnetic waves and light, the governing equation is the Maxwell's equations. General numerical methods such as the finite element method [13–16], can always be used, but it is possible to develop more efficient special computational methods by taking advantage of the available geometric features. For crossed arrays of cylinders, each layer is invariant in one spatial variable. In an x-invariant layer, if the wave field is decomposed into Fourier modes in x, then these modes are uncoupled within the layer. This implies that although the problem is truly three dimensional, the wave field in each layer can be resolved by solving a sequence of two-dimensional (2D) problems corresponding to different Fourier modes in one spatial direction. If the structure has many layers in the z direction and some of these layers are identical, it is desirable to avoid duplicated calculations in identical layers. If the cylinders have circular cross sections, it is also possible to develop efficient semi-analytic method based on cylindrical wave expansions.

For crossed arrays of circular cylinders, a semi-analytic method based on scattering matrices and cylindrical wave expansions was developed by Smith *et al.* [17] and Yasumoto and Jia [18]. The scattering matrices are used to avoid duplicated computations in identical layers. Cylindrical wave expansions are used for calculating the scattering matrix of each layer. In both works, sophisticated lattice sums techniques [19] are needed to take care of the periodic array of cylinders in each layer. For the same structures, we developed a semi-analytic method based on Dirichlet-to-Neumann (DtN) maps [20]. The DtN-map approach also uses cylindrical wave expansions, but it avoids the tedious lattice sums and is more efficient.

In this paper, we develop a simpler and more efficient semi-analytic method for analyzing crossed arrays of circular cylinders. Instead of the DtN maps, we use operators that map two tangential components of the electromagnetic field to two different tangential components (the T2T operators). Since the tangential components are continuous across a surface, the T2T operators are also continuous across interfaces. This leads a number of simplifications compared with the DtN-map method [20]. Cylindrical wave expansions are also used, but as in the DtN-map method, lattice sums are not needed, since the T2T operators are constructed starting from the unit cells. Numerical examples are used to validate the method and illustrate its accuracy and efficiency.

2 Formulation

For linear electromagnetic waves in isotropic media without sources, the governing equations in the frequency domain are the Maxwell's equations:

$$\nabla\times\mathbf{E}=ik_0\mu\tilde{\mathbf{H}},\quad \nabla\times\tilde{\mathbf{H}}=-ik_0\varepsilon\mathbf{E},\tag{2.1}$$

where $\mathbf{E}$ is the electric field, $\tilde{\mathbf{H}}$ is the magnetic field multiplied by free space impedance, $k_0=\omega/c$ is the free space wavenumber, ω is the angular frequency, c is the speed of light in vacuum, ε is the relative permittivity, μ is the relative permeability, and the time dependence is assumed to be $\exp(-i\omega t)$. We consider a biperiodic structure given in $0<z<D$, and bounded by homogeneous media in $z<0$ and $z>D$, where the z axis is assumed to be in the vertical direction. For the top and bottom homogeneous media, we assume $\{\varepsilon,\mu\}=\{\varepsilon^{(1)},\mu^{(1)}\}$ for $z>D$ and $\{\varepsilon,\mu\}=\{\varepsilon^{(2)},\mu^{(2)}\}$ for $z<0$, where $\varepsilon^{(1)}$, $\mu^{(1)}$, $\varepsilon^{(2)}$ and $\mu^{(2)}$ are constants. The structure consists of M layers separated by $0=z_0<z_1<\cdots<z_M=D$. Two four-layer examples are shown in Fig. 1. The mth layer is given by $z_{m-1}<z<z_m$ for $1\le m\le M$. In each layer, the structure is either periodic in x and invariant in y, or periodic in y and invariant in x, with period L in both directions. In particular, we will analyze crossed arrays of circular cylinders, where the mth layer consists of a periodic array of circular cylinders parallel to either x or y, and surrounded by a homogeneous medium.

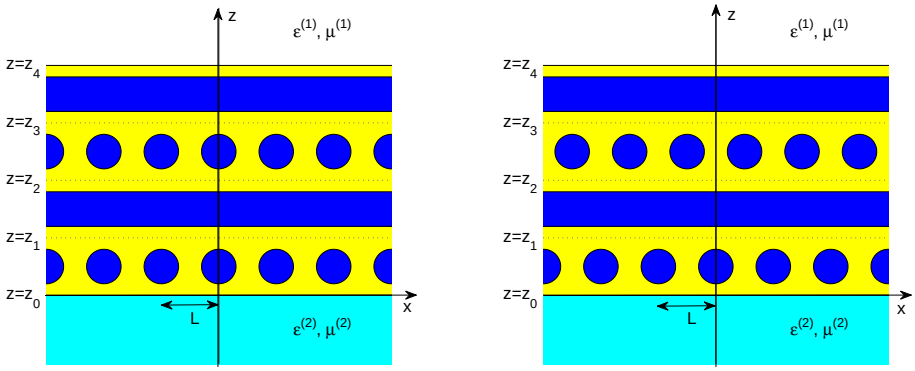

Figure 1: Side views in xz plane of four-layer structures with crossed arrays of circular cylinders. Left: regular arrays; Right: woodpile arrays.

For $z>D$, we specify a plane incident wave $\{\mathbf{E}^{(i)},\tilde{\mathbf{H}}^{(i)}\}$ with the wave vector $(\alpha_0,\beta_0,-\gamma_{00}^{(1)})$, where α_0 and β_0 are real and

$$\gamma_{00}^{(1)}=\sqrt{k_0^2\varepsilon^{(1)}\mu^{(1)}-\alpha_0^2-\beta_0^2}.\tag{2.2}$$

The objective is to calculate the reflected wave $\{\mathbf{E}^{(r)},\tilde{\mathbf{H}}^{(r)}\}$ in the top ($z>D$) and the transmitted wave $\{\mathbf{E}^{(t)},\tilde{\mathbf{H}}^{(t)}\}$ in the bottom ($z<0$). Due to the periodicity of the structure and the specific form of the incident wave, the electromagnetic field is quasi-periodic in x and y. That is, the wave field multiplied by $e^{-i(\alpha_0x+\beta_0y)}$ is periodic in x and y with period L. In particular, the reflected and transmitted waves can be expanded in plane waves

with wave vectors $(\alpha_j,\beta_k,\gamma_{jk}^{(1)})$ and $(\alpha_j,\beta_k,-\gamma_{jk}^{(2)})$, respectively, where

$$\alpha_j=\alpha_0+\frac{2\pi j}{L},\quad \beta_k=\beta_0+\frac{2\pi k}{L}, \tag{2.3}$$

$$\gamma_{jk}^{(l)}=\sqrt{k_0^2\varepsilon^{(l)}\mu^{(l)}-\alpha_j^2-\beta_k^2},\quad l=1,2. \tag{2.4}$$

The complex square root in (2.2) and (2.4) must be defined such that either $\mathrm{Im}(\gamma_{jk}^{(l)})>0$ or $\gamma_{jk}^{(l)}$ is real and non-negative. The plane wave components with wave vectors $(\alpha_j,\beta_k,\gamma_{jk}^{(1)})$ and $(\alpha_j,\beta_k,-\gamma_{jk}^{(2)})$ are the (j,k)-th reflection and transmission orders, respectively.

For a given wavevector, there are two linearly independent plane waves. For a particular plane wave, if the coefficients of two properly chosen field components are known, the coefficients of the other four components can be determined. In particular, if the x and y components of the transmitted wave are given as

$$\boldsymbol{u}^{(t)}=\sum_{jk}\boldsymbol{a}_{jk}^{(t)}\exp[i(\alpha_j x+\beta_k y-\gamma_{jk}^{(2)}z)],\quad z<0,$$

$$\boldsymbol{v}^{(t)}=\sum_{jk}\boldsymbol{b}_{jk}^{(t)}\exp[i(\alpha_j x+\beta_k y-\gamma_{jk}^{(2)}z)],\quad z<0,$$

where

$$\boldsymbol{u}=\begin{bmatrix}E_x\\ \tilde{H}_x\end{bmatrix},\quad \boldsymbol{v}=\begin{bmatrix}E_y\\ \tilde{H}_y\end{bmatrix}, \tag{2.5}$$

then the coefficients $\boldsymbol{a}_{jk}^{(t)}$ and $\boldsymbol{b}_{jk}^{(t)}$ (column vectors of length 2) are related to each other by

$$\boldsymbol{a}_{jk}^{(t)}+B_{jk}^{(t)}\boldsymbol{b}_{jk}^{(t)}=0,$$

where

$$B_{jk}^{(t)}=\frac{1}{\eta_k^{(2)}}\begin{bmatrix}\alpha_j\beta_k & k_0\mu^{(2)}\gamma_{jk}^{(2)}\\ -k_0\varepsilon^{(2)}\gamma_{jk}^{(2)} & \alpha_j\beta_k\end{bmatrix}$$

and $\eta_k^{(2)}=k_0^2\varepsilon^{(2)}\mu^{(2)}-\beta_k^2$. For the above matrix to exist, it is necessary to assume that $\eta_k^{(2)}\neq 0$ for all k. In that case, we can define an operator $\mathcal{B}^{(t)}$ [20], such that

$$\boldsymbol{u}^{(t)}+\mathcal{B}^{(t)}\boldsymbol{v}^{(t)}=\boldsymbol{0},\quad z<0.$$

Since the transmitted field is the total field for $z<0$, and $\boldsymbol{u}$ and $\boldsymbol{v}$ are continuous at $z=0$, we have

$$\boldsymbol{u}+\mathcal{B}^{(t)}\boldsymbol{v}=\boldsymbol{0},\quad z=0. \tag{2.6}$$

The above serves as a boundary condition at $z=0$. It is referred to as the downward radiation condition.

Similarly, we can define an operator $\mathcal{B}^{(r)}$ for the reflected wave based on the 2×2 matrices

$$B_{jk}^{(r)}=\frac{1}{\eta_k^{(1)}}\begin{bmatrix}\alpha_j\beta_k & -k_0\mu^{(1)}\gamma_{jk}^{(1)}\\ k_0\varepsilon^{(1)}\gamma_{jk}^{(1)} & \alpha_j\beta_k\end{bmatrix},$$

where $\eta_k^{(1)}=k_0^2\varepsilon^{(1)}\mu^{(1)}-\beta_k^2$ are assumed to be non-zero, so that the boundary condition at $z=D$ is

$$\boldsymbol{u}+\mathcal{B}^{(r)}\boldsymbol{v}=\left[\boldsymbol{u}^{(i)}+\mathcal{B}^{(r)}\boldsymbol{v}^{(i)}\right]_{z=D^+},\quad z=D. \tag{2.7}$$

More details can be found in [20]. The boundary conditions (2.6) and (2.7) are valid for all but one discrete sequence of frequencies where $\eta_k^{(1)}$ or $\eta_k^{(2)}$ is zero for some integer k. If we use an operator that maps $\boldsymbol{u}$ to $\boldsymbol{v}$ (instead of $\boldsymbol{v}$ to $\boldsymbol{u}$) to define the boundary conditions, a similar difficulty appears when $\sigma_j^{(l)}=k_0^2\varepsilon^{(l)}\mu^{(l)}-\alpha_j^2$ becomes zero for $l=1$ or 2. Using operators between different linear combinations of the four field components E_x, E_y, $\tilde{H}_x$ and $\tilde{H}_y$, it is possible to establish boundary conditions that are valid for all frequencies. The details are given in Section 6.

The quasi-periodic condition of the electromagnetic field can be written as

$$\phi(x+L,y,z)=e^{i\alpha_0 L}\phi(x,y,z),\quad \phi(x,y+L,z)=e^{i\beta_0 L}\phi(x,y,z), \tag{2.8}$$

where ϕ is any component of the electromagnetic field. Therefore, using Eqs. (2.6), (2.7) and (2.8), the boundary value problem is now formulated on the domain

$$\Omega=\{(x,y,z)\,|\,0<x<L,\ 0<y<L,\ 0<z<D\}. \tag{2.9}$$

3 Marching schemes

A general numerical method, such as the finite element method [13–16], can be used to solve the boundary value problem (2.1), (2.6)-(2.8) formulated on Ω. However, it is possible to develop more efficient computational methods by utilizing the special geometric features of the structures. For layered structures, it is often advantageous to use an operator marching (OM) scheme [21–28] to avoid repeated calculations in different layers with identical or similar profiles. This is particularly true when the layers are relatively simple, such as arrays of circular cylinders, so that semi-analytic methods can be used.

For a multilayer structure where the layers are separated by z_0, z_1,$\cdots$, and z_M, and the incident wave is given in the top, an OM scheme marches some operators from $z=0^-$ to $z=D^+$, and determines the reflected and transmitted waves afterwards. One approach is to use the scattering (i.e., reflection and transmission) operators based on a decomposition of the wave field into upward and downward components [17, 18, 21–23]. At a fixed z, the reflection operator maps the downward component to the upward component, but it is discontinuous at z_m if the media above and below z_m are different. As a result, the OM scheme for reflection and transmission operators must manipulate these

two operators from z_{m-1}^+ to z_m^- (for $m=1,2,\cdots,M$) and from z_m^- to z_m^+ (for $m=0,1,\cdots,M$). The step from z_{m-1}^+ to z_m^- requires the 2×2 scattering matrix (with operator entries) of the layer. Furthermore, when the directional wave field components are expanded in Fourier series, each operator is represented by an infinite matrix. For structures where the layers are composed of arrays of circular cylinders, cylindrical wave expansions with lattice sums techniques have been used to calculate the scattering matrices of the layers [17,18].

In our previous work [20], an OM scheme was formulated based on the Dirichlet-to-Neumann (DtN) operator and a related propagation operator. For a fixed z, the DtN operator maps the wave field to its z derivative. The wave field decomposition is not needed, but the DtN operator is also discontinuous at horizontal material interfaces. Similar to the scheme based on scattering operators, the DtN scheme also requires two different kinds of steps: the step for a layer (from z_{m-1}^+ to z_m^-) and the step for an interface (from z_m^- to z_m^+). In addition, the step from z_{m-1}^+ to z_m^- requires a 2×2 matrix DtN operator of the layer. Compared with the scattering matrix formalism [17,18], the DtN approach is more efficient, since the DtN operator of the layer can be constructed from the same operator of a unit cell, and this process does not need to evaluate lattice sums.

To avoid the discontinuity of scattering and DtN operators at horizontal material interfaces, we can use operators that manipulate the tangential (i.e. x and y) field components which are continuous. One approach is to use the impedance or admittance operator that relate the tangential electric field components to the tangential magnetic field components [23]. Since the layers are invariant in either x or y, it is convenient to group the tangential components according to the directions. In the following, we present an OM scheme based on an operator $\mathcal{B}$ that links the two x components with the two y components. For a fixed $z_*\geq z_0$, the operator $\mathcal{B}$ satisfies

$$\mathcal{B}(z_*)\boldsymbol{v}=-\boldsymbol{u},\quad \text{at}\quad z=z_*, \tag{3.1}$$

where $\boldsymbol{u}$ and $\boldsymbol{v}$ are the x and y components of an arbitrary electromagnetic field satisfying the Maxwell's equations (2.1) for $z<z_*$, the downward radiation condition (2.6), and the quasi-periodic condition (2.8). The reflected wave can be determined when $\mathcal{B}$ at $z_M=D$ is obtained. To find the transmitted wave, we need the propagation operator $\mathcal{W}$ satisfying

$$\mathcal{W}(z_*)\boldsymbol{v}|_{z=z_*}=\boldsymbol{v}|_{z=z_0}. \tag{3.2}$$

At $z=z_0$, these two operators are given by

$$\mathcal{B}(z_0)=\mathcal{B}^{(t)},\quad \mathcal{W}(z_0)=\mathcal{I},$$

where $\mathcal{B}^{(t)}$ is the operator given in Eq. (2.6) and $\mathcal{I}$ is the identity operator. The main step of the OM scheme is to march $\mathcal{B}$ and $\mathcal{W}$ from z_{m-1} to z_m for $m=1,2,\cdots,M$. If $\mathcal{B}(z_M)$ and $\mathcal{W}(z_M)$ are known, we can find the total field at z_M by solving

$$\left[-\mathcal{B}(z_M)+\mathcal{B}^{(r)}\right]\boldsymbol{v}|_{z=z_M}=\left[\boldsymbol{u}^{(i)}+\mathcal{B}^{(r)}\boldsymbol{v}^{(i)}\right]_{z=D^+}. \tag{3.3}$$

The reflected wave can be obtained by subtracting the incident field. The transmitted wave can be easily evaluated using $\mathcal{W}(z_M)$:

$$\boldsymbol{v}|_{z=z_0} = \mathcal{W}(z_M)\boldsymbol{v}|_{z=z_M}. \tag{3.4}$$

We note that if there is a non-zero electromagnetic field satisfying the Maxwell's equations (2.1) for $z<z_*$, the boundary conditions (2.6) and (2.8), and $\boldsymbol{v}=\boldsymbol{0}$ at $z=z_*$, then $\mathcal{B}$ and $\mathcal{W}$ cannot be defined at z_*. This could happen for some special frequencies. In Section 6, we present an approach to avoid this difficulty.

To march the operators through a layer, i.e., from z_{m-1} to z_m, we need a local T2T operator $\mathcal{N}^{(m)}$ defined for the tangential field components on the two horizontal interfaces at z_{m-1} and z_m. It satisfies

$$\mathcal{N}^{(m)}\begin{bmatrix}\boldsymbol{v}(z_{m-1})\\ \boldsymbol{v}(z_m)\end{bmatrix} = \begin{bmatrix}\mathcal{N}_{11}^{(m)} & \mathcal{N}_{12}^{(m)}\\ \mathcal{N}_{21}^{(m)} & \mathcal{N}_{22}^{(m)}\end{bmatrix}\begin{bmatrix}\boldsymbol{v}(z_{m-1})\\ \boldsymbol{v}(z_m)\end{bmatrix} = \begin{bmatrix}\boldsymbol{u}(z_{m-1})\\ \boldsymbol{u}(z_m)\end{bmatrix}. \tag{3.5}$$

In the above, $\mathcal{N}^{(m)}$ is given as a 2×2 matrix where each entry is an operator acting on vectors of two functions of x and y. It is defined for any electromagnetic field satisfying Eqs. (2.1) and (2.8) for $z_{m-1}<z<z_m$. The definition may fail, if there is a non-zero quasi-periodic electromagnetic field satisfying the zero boundary conditions $\boldsymbol{v}(z_{m-1})=\boldsymbol{v}(z_m)=\boldsymbol{0}$. An alternative OM scheme without this problem is presented in Section 6. Using the definitions of $\mathcal{B}$, $\mathcal{W}$ and $\mathcal{N}^{(m)}$, it is easy to derive the following marching formulae:

$$\mathcal{Z} = [\mathcal{B}(z_{m-1}) + \mathcal{N}_{11}^{(m)}]^{-1}\mathcal{N}_{12}^{(m)}, \tag{3.6}$$

$$\mathcal{B}(z_m) = \mathcal{N}_{21}^{(m)}\mathcal{Z} - \mathcal{N}_{22}^{(m)}, \tag{3.7}$$

$$\mathcal{W}(z_m) = -\mathcal{W}(z_{m-1})\mathcal{Z}. \tag{3.8}$$

Notice that $\mathcal{Z}$ is the projection operator that maps $\boldsymbol{v}(z_m)$ to $-\boldsymbol{v}(z_{m-1})$.

The above OM scheme based on $\mathcal{B}$, $\mathcal{W}$ and $\mathcal{N}^{(m)}$ is applicable to general multilayered biperiodic structures. In principle, a general numerical method can be used to calculate the local T2T operator $\mathcal{N}^{(m)}$. The method is especially useful if there is a partial periodicity in the z direction, and when the horizontal periods (in x and y) are not very large compared with the wavelength, so that the operators can be approximated by relatively small matrices. In Section 5, we present an efficient semi-analytic method to construct $\mathcal{N}^{(m)}$.

4 Representations in Fourier space

For a given z, a component ϕ of the electromagnetic field satisfies the quasi-periodic condition (2.8), and it can be expanded in Fourier series as

$$\phi(x,y,z) = \sum_{j,k=-\infty}^{\infty} \hat{\phi}_{jk}(z)e^{i(\alpha_j x+\beta_k y)}. \tag{4.1}$$

In practice, we truncate the Fourier series to N terms in each direction, that is, j and k are chosen from $-N/2$ to $N/2-1$ if N is even and from $-(N-1)/2$ to $(N-1)/2$ if N is odd. These N^2 coefficients can be put together in a column vector $\hat{\phi}$. For example, we can put the N coefficients with the same k together as a column vector of length N, then put all these N vectors together as one big vector of length N^2.

If a linear operator $\mathcal{T}$ acts on quasi-periodic functions and the results are also quasi-periodic, then it can be approximated by an $N^2\times N^2$ matrix. From the Fourier series

$$\mathcal{T}\{e^{i(\alpha_j x+\beta_k y)}\}=\sum_{l,m=-\infty}^{\infty} T_{lm}^{jk} e^{i(\alpha_l x+\beta_m y)}, \tag{4.2}$$

we immediately get the Fourier series of $\psi=\mathcal{T}\phi$:

$$\psi=\sum_{l,m=-\infty}^{\infty}\left(\sum_{j,k=\infty}^{\infty} T_{lm}^{jk}\hat{\phi}_{jk}\right)e^{i(\alpha_l x+\beta_m y)}=\sum_{l,m=-\infty}^{\infty}\hat{\psi}_{lm}e^{i(\alpha_l x+\beta_m y)}. \tag{4.3}$$

This leads the relation $\hat{\psi}=\hat{\mathcal{T}}\hat{\phi}$, where $\hat{\psi}$ is defined as $\hat{\phi}$ with the same ordering of the indices, $\hat{\mathcal{T}}$ is a matrix with row and column indices given by (l,m) and (j,k), respectively.

Due to the vector nature of our problem, the operators $\mathcal{B}$ and $\mathcal{W}$ act on column vectors of two quasi-periodic functions. Therefore, the operator $\mathcal{B}$ is in fact a 2×2 matrix where each entry is an operator. In the Fourier space and after the truncation of the Fourier series, the operators $\mathcal{B}$ and $\mathcal{W}$ are approximately represented by $(2N^2)\times(2N^2)$ matrices $\hat{\mathcal{B}}$ and $\hat{\mathcal{W}}$. Similarly, the local T2T operator $\mathcal{N}^{(m)}$ is approximated by a $(4N^2)\times(4N^2)$ matrix $\hat{\mathcal{N}}^{(m)}$. The operators $\mathcal{B}^{(t)}$ and $\mathcal{B}^{(r)}$ that appear in the boundary conditions (2.6) and (2.7) are represented by $(2N^2)\times(2N^2)$ matrices $\hat{\mathcal{B}}^{(t)}$ and $\hat{\mathcal{B}}^{(r)}$, and they are 2×2 block matrices where each block is an $N^2\times N^2$ diagonal matrix. In fact, the four entries of the matrix $B_{jk}^{(t)}$ give the diagonal entries of the four block matrices in $\hat{\mathcal{B}}^{(t)}$ with an index corresponding to (j,k).

The equations in Section 4 remain valid if we replace the wave field components and the operators by the corresponding vectors and matrices in Fourier space.

5 T2T operators

In this section, we present the steps for constructing the local T2T operators $\mathcal{N}^{(m)}$ for layers with a periodic array of circular cylinders. Without loss of generality, we consider the first two layers, assume the first layer is y-invariant and the second layer is x-invariant.

In the first layer, if the electromagnetic field is expanded in Fourier series in y, the different Fourier components are uncoupled, and they can be studied as independent 2D problems. More precisely, we have

$$\boldsymbol{u}=\sum_{k=-\infty}^{\infty}\boldsymbol{u}_k,\quad \boldsymbol{v}=\sum_{k=-\infty}^{\infty}\boldsymbol{v}_k,\quad \boldsymbol{w}=\sum_{k=-\infty}^{\infty}\boldsymbol{w}_k \tag{5.1}$$

for $z_0<z<z_1$, where $\boldsymbol{w}=(E_z,\tilde{H}_z)^T$ is a column vector of the two z components, $\boldsymbol{u}_k$, $\boldsymbol{v}_k$ and $\boldsymbol{w}_k$ depend on y as $e^{i\beta_k y}$. For each k, we first construct a T2T operator $\mathcal{N}_k$ in the physical space, then transform it to the Fourier space to obtain $\hat{\mathcal{N}}_k$. Finally, we assemble $\hat{\mathcal{N}}_k$ (for all k) together to form $\hat{\mathcal{N}}^{(1)}$. Notice that $\hat{\mathcal{N}}_k$ is approximated by a $(4N)\times(4N)$ matrix. In the physical space, the operator $\mathcal{N}_k$ is also approximated by a $(4N)\times(4N)$ matrix.

To find $\mathcal{N}_k$, we consider a 2D unit cell in the xz plane:

$$\Omega_1=\left\{(x,z)\;\middle|\; x_c-\frac{L}{2}<x<x_c+\frac{L}{2},\, z_0<z<z_1\right\},$$

such that the center of the circular cylinder closest to the z axis is (x_c,z_c), where typically $z_c=(z_0+z_1)/2$. Since the x-coordinates of the cylinders in different y-invariant layers can be different in general, we introduce a horizontal shift x_c. Within the unit cell, we use a polar coordinate system (r,θ) centered at (x_c,z_c), and expand the field in vector cylindrical waves as

$$\boldsymbol{v}_k=\sum_{m=-\infty}^{\infty}\boldsymbol{\Phi}_m(r)\boldsymbol{b}_m e^{i(m\theta+\beta_k y)}, \tag{5.2}$$

where $\boldsymbol{\Phi}_m$ is a 2×2 matrix and $\boldsymbol{b}_m$ is a column vector of two arbitrary coefficients. The explicit form of $\boldsymbol{\Phi}_m$ is given in [29], it depends on the radius and the refractive index of the cylinder, and the refractive index of the surrounding medium in the unit cell. The other four components of the electromagnetic field are related to $\boldsymbol{v}_k$. From the Maxwell's equations, it is easy to show that

$$\boldsymbol{u}_k=\frac{i}{\eta_k}\left(\beta_k\frac{\partial\boldsymbol{v}_k}{\partial x}+k_0\mathbf{L}\frac{\partial\boldsymbol{v}_k}{\partial z}\right), \tag{5.3}$$

$$\boldsymbol{w}_k=\frac{i}{\eta_k}\left(\beta_k\frac{\partial\boldsymbol{v}_k}{\partial z}-k_0\mathbf{L}\frac{\partial\boldsymbol{v}_k}{\partial x}\right), \tag{5.4}$$

where $\eta_k=k_0^2\varepsilon\mu-\beta_k^2$ is assumed to be non-zero, and

$$\mathbf{L}=\begin{bmatrix}0 & -\mu\\ \varepsilon & 0\end{bmatrix}.$$

Therefore, we can expand $\boldsymbol{u}_k$ and $\boldsymbol{w}_k$ in cylindrical waves with the same coefficients $\{\boldsymbol{b}_m:-\infty<m<\infty\}$.

On the boundary of Ω_1, we choose $2N+2N'$ points, with N and N' points on the horizontal and vertical edges, respectively. The x and z coordinates of the points on the horizontal and vertical edges are given by

$$x_l=x_c+\left(\frac{l-0.5}{N}-\frac{1}{2}\right)L,\quad l=1,2,\cdots,N,\quad\text{and}$$

$$z_{0,l}=z_0+\frac{l-0.5}{N'}(z_1-z_0),\quad l=1,2,\cdots,N',$$

respectively. We also truncate the vector cylindrical wave expansion (5.2) to retain $2(N+N')$ terms, i.e. for $-(N+N')\leq m\leq N+N'-1$. If we evaluate the truncated version of (5.2) at the $2(N+N')$ points on the boundary of Ω_1, we obtain a $4(N+N')\times 4(N+N')$ matrix $\Theta_k^{(1)}$ linking $\boldsymbol{v}_k$ on the boundary to the coefficients:

$$\begin{bmatrix} \boldsymbol{v}_k^{(0)} \\ \boldsymbol{v}_k^{(l)} \\ \boldsymbol{v}_k^{(r)} \\ \boldsymbol{v}_k^{(1)} \end{bmatrix} = \Theta_k^{(1)} \vec{\boldsymbol{b}},$$

where $\vec{\boldsymbol{b}}$ is a vector for $\{\boldsymbol{b}_m : -(N+N')\leq m\leq N+N'-1\}$, $\boldsymbol{v}_k^{(0)}$, $\boldsymbol{v}_k^{(l)}$, $\boldsymbol{v}_k^{(r)}$ and $\boldsymbol{v}_k^{(1)}$ are column vectors for $\boldsymbol{v}_k$ at the discrete points on the bottom, left, right and top edges of Ω_1. The cylindrical wave expansions for $\boldsymbol{u}_k$ and $\boldsymbol{w}_k$ are similarly truncated. Evaluating the truncated expansions of $\boldsymbol{u}_k$ and $\boldsymbol{w}_k$ on the horizontal and vertical edges of Ω_1, respectively, we obtain another $4(N+N')\times 4(N+N')$ matrix $\Theta_k^{(2)}$, such that

$$\begin{bmatrix} \boldsymbol{u}_k^{(0)} \\ \boldsymbol{w}_k^{(l)} \\ \boldsymbol{w}_k^{(r)} \\ \boldsymbol{u}_k^{(1)} \end{bmatrix} = \Theta_k^{(2)} \vec{\boldsymbol{b}},$$

where $\boldsymbol{u}_k^{(0)}$, $\boldsymbol{w}_k^{(l)}$, $\boldsymbol{w}_k^{(r)}$ and $\boldsymbol{u}_k^{(1)}$ are vectors defined as those for $\boldsymbol{v}_k$. Eliminating $\vec{\boldsymbol{b}}$, we have a $4(N+N')\times 4(N+N')$ matrix $\Theta_k = \Theta_k^{(2)}[\Theta_k^{(1)}]^{-1}$, such that

$$\Theta_k \begin{bmatrix} \boldsymbol{v}_k^{(0)} \\ \boldsymbol{v}_k^{(l)} \\ \boldsymbol{v}_k^{(r)} \\ \boldsymbol{v}_k^{(1)} \end{bmatrix} = \begin{bmatrix} \boldsymbol{u}_k^{(0)} \\ \boldsymbol{w}_k^{(l)} \\ \boldsymbol{w}_k^{(r)} \\ \boldsymbol{u}_k^{(1)} \end{bmatrix}. \tag{5.5}$$

For the cylinder with cross section Ω_1, $\boldsymbol{v}_k$ and $\boldsymbol{u}_k$ are tangential field components on the horizontal boundaries, and $\boldsymbol{v}_k$ and $\boldsymbol{w}_k$ are tangential field components on the vertical boundaries, therefore Θ_k above maps tangential field components to tangential field components, and it is the T2T operator of the unit cell for a field with the given $e^{i\beta_k y}$ dependence on y.

Since the field is quasi-periodic in the x direction, we have

$$\boldsymbol{v}_k^{(r)} = e^{i\alpha_0 L}\boldsymbol{v}_k^{(l)}, \quad \boldsymbol{w}_k^{(r)} = e^{i\alpha_0 L}\boldsymbol{w}_k^{(l)}. \tag{5.6}$$

Writing down Θ_k in 4×4 blocks and using the above quasi-periodic condition, we can eliminate $\boldsymbol{v}_k^{(l)}$, $\boldsymbol{v}_k^{(r)}$, $\boldsymbol{w}_k^{(l)}$ and $\boldsymbol{w}_k^{(r)}$, and find $\mathcal{N}_k$ satisfying

$$\mathcal{N}_k \begin{bmatrix} \boldsymbol{v}_k^{(0)} \\ \boldsymbol{v}_k^{(1)} \end{bmatrix} = \begin{bmatrix} \boldsymbol{u}_k^{(0)} \\ \boldsymbol{u}_k^{(1)} \end{bmatrix}. \tag{5.7}$$

The above $\mathcal{N}_k$ is a $(4N)\times(4N)$ matrix, it is the T2T operator of the layer in physical space for a wave field that depends on y as $e^{i\beta_k y}$.

To obtain the Fourier representation of $\mathcal{N}_k$, we make use of the discrete Fourier transform. Since the y dependence is fixed as $e^{i\beta_k y}$, we only need the discrete Fourier transform in x. For a scalar quasi-periodic function $\phi(x)$, we have the approximate relation

$$\phi(x_l)=\sum_{j=-N/2}^{N/2-1}\hat{\phi}_j e^{i\alpha_j x_l},\quad l=1,2,\cdots,N, \tag{5.8}$$

where $\hat{\phi}_j$ are the Fourier coefficients of ϕ, N is assumed to be even, otherwise j is from $-(N-1)/2$ to $(N-1)/2$. This gives rise to an $N\times N$ matrix relating a vector of ϕ at N points in the physical space with a vector for its N Fourier coefficients. Such a relation is valid for the x and y field components in $\boldsymbol{u}_k$ and $\boldsymbol{v}_k$ (at both z_0 and z_1), respectively. Therefore, we can insert this linear relation into Eq. (5.7) and obtain $\hat{\mathcal{N}}_k$ satisfying

$$\hat{\mathcal{N}}_k\begin{bmatrix}\hat{\boldsymbol{v}}_k^{(0)}\\ \hat{\boldsymbol{v}}_k^{(1)}\end{bmatrix}=\begin{bmatrix}\hat{\boldsymbol{u}}_k^{(0)}\\ \hat{\boldsymbol{u}}_k^{(1)}\end{bmatrix}, \tag{5.9}$$

where $\hat{\boldsymbol{u}}_k^{(0)}$ is a vector of length $2N$ for the Fourier coefficients of E_x and $\tilde{H}_x$ at $z=z_0$ and fixed k, etc. Finally, we simply put $\hat{\mathcal{N}}_k$ for all k into a $(4N^2)\times(4N^2)$ matrix to form the T2T operator of the layer in Fourier space. This gives rise to $\hat{\mathcal{N}}^{(1)}$ satisfying

$$\hat{\mathcal{N}}^{(1)}\begin{bmatrix}\hat{\boldsymbol{v}}(z_0)\\ \hat{\boldsymbol{v}}(z_1)\end{bmatrix}=\begin{bmatrix}\hat{\boldsymbol{u}}(z_0)\\ \hat{\boldsymbol{u}}(z_1)\end{bmatrix}. \tag{5.10}$$

For the second layer ($z_1<z<z_2$) which is invariant in x and periodic in y with period L, the local T2T operator $\hat{\mathcal{N}}^{(2)}$ can be constructed using a similar but slightly different procedure. With some abuse of notations, we follow the Fourier expansion in x and decompose the wave field as

$$\boldsymbol{u}=\sum_{j=-\infty}^{\infty}\boldsymbol{u}_j,\quad \boldsymbol{v}=\sum_{j=-\infty}^{\infty}\boldsymbol{v}_j,\quad \boldsymbol{w}=\sum_{j=-\infty}^{\infty}\boldsymbol{w}_j \tag{5.11}$$

for $z_1<z<z_2$, where $\boldsymbol{u}_j$, $\boldsymbol{v}_j$ and $\boldsymbol{w}_j$ depend on x as $e^{i\alpha_j x}$. For a given $\boldsymbol{u}_j$, the corresponding y and z components can be evaluated by the following equations:

$$\boldsymbol{v}_j=\frac{i}{\sigma_j}\left[\alpha_j\frac{\partial\boldsymbol{u}_j}{\partial y}-k_0\mathbf{L}\frac{\partial\boldsymbol{u}_j}{\partial z}\right], \tag{5.12}$$

$$\boldsymbol{w}_j=\frac{i}{\sigma_j}\left[\alpha_j\frac{\partial\boldsymbol{u}_j}{\partial z}+k_0\mathbf{L}\frac{\partial\boldsymbol{u}_j}{\partial y}\right], \tag{5.13}$$

where $\sigma_j=k_0^2\varepsilon\mu-\alpha_j^2$ is assumed to be non-zero.

In the yz plane, we introduce a 2D unit cell for the second layer:

$$\Omega_2 = \left\{ (y,z) \,\middle|\, y_c - \frac{L}{2} < y < y_c + \frac{L}{2},\ z_1 < z < z_2 \right\},$$

such that the center of the cylinder is (y_c, z_c). With a polar coordinate system centered at (y_c, z_c), we can expand the field in cylindrical waves as before. When the horizontal and vertical edges of the unit cell are discretized by N and N' points, respectively, and cylindrical wave expansions are properly truncated, we obtain the following two equations

$$\begin{bmatrix} \boldsymbol{u}_j^{(1)} \\ \boldsymbol{u}_j^{(l)} \\ \boldsymbol{u}_j^{(r)} \\ \boldsymbol{u}_j^{(2)} \end{bmatrix} = \Theta_j^{(1)} \vec{\boldsymbol{b}}, \quad \begin{bmatrix} \boldsymbol{v}_j^{(1)} \\ \boldsymbol{w}_j^{(l)} \\ \boldsymbol{w}_j^{(r)} \\ \boldsymbol{v}_j^{(2)} \end{bmatrix} = \Theta_j^{(2)} \vec{\boldsymbol{b}},$$

This leads to $\Theta_j = \Theta_j^{(1)} [\Theta_j^{(2)}]^{-1}$ such that

$$\Theta_j \begin{bmatrix} \boldsymbol{v}_j^{(1)} \\ \boldsymbol{w}_j^{(l)} \\ \boldsymbol{w}_j^{(r)} \\ \boldsymbol{v}_j^{(2)} \end{bmatrix} = \begin{bmatrix} \boldsymbol{u}_j^{(1)} \\ \boldsymbol{u}_j^{(l)} \\ \boldsymbol{u}_j^{(r)} \\ \boldsymbol{u}_j^{(2)} \end{bmatrix}. \tag{5.14}$$

The quasi-periodic condition in the y direction gives

$$\boldsymbol{u}_j^{(r)} = e^{i\beta_0 L} \boldsymbol{u}_j^{(l)}, \quad \boldsymbol{w}_j^{(r)} = e^{i\beta_0 L} \boldsymbol{w}_j^{(l)}. \tag{5.15}$$

Eliminating the components on the vertical edges from (5.14), we obtain

$$\mathcal{N}_j \begin{bmatrix} \boldsymbol{v}_j^{(1)} \\ \boldsymbol{v}_j^{(2)} \end{bmatrix} = \begin{bmatrix} \boldsymbol{u}_j^{(1)} \\ \boldsymbol{u}_j^{(2)} \end{bmatrix}. \tag{5.16}$$

In Fourier space, the above becomes

$$\hat{\mathcal{N}}_j \begin{bmatrix} \hat{\boldsymbol{v}}_j^{(1)} \\ \hat{\boldsymbol{v}}_j^{(2)} \end{bmatrix} = \begin{bmatrix} \hat{\boldsymbol{u}}_j^{(1)} \\ \hat{\boldsymbol{u}}_j^{(2)} \end{bmatrix}. \tag{5.17}$$

Assembling $\tilde{\mathcal{N}}_j$ for all j in one matrix, we obtain the T2T operator $\hat{\mathcal{N}}^{(2)}$ satisfying

$$\hat{\mathcal{N}}^{(2)} \begin{bmatrix} \hat{\boldsymbol{v}}(z_1) \\ \hat{\boldsymbol{v}}(z_2) \end{bmatrix} = \begin{bmatrix} \hat{\boldsymbol{u}}(z_1) \\ \hat{\boldsymbol{u}}(z_2) \end{bmatrix}. \tag{5.18}$$

6 Robust marching scheme

As mentioned in previous sections, the OM scheme based on the T2T operator $\mathcal{B}$, the propagation operator $\mathcal{W}$ and the local T2T operator $\mathcal{N}^{(m)}$, could break down at frequencies where some of these operators cannot be defined. In this section, we present a more robust scheme that in principle should work for all frequencies. The idea is similar to those used in domain decomposition methods [30] and in a 2D OM scheme developed by Ehrhardt *et al.* [31].

Let $\boldsymbol{u}'$ and $\boldsymbol{v}'$ be given by

$$\boldsymbol{u}'=\begin{bmatrix}E_x+\rho\tilde{H}_y\\ \tilde{H}_x-\rho E_y\end{bmatrix},\quad \boldsymbol{v}'=\begin{bmatrix}E_y+\rho\tilde{H}_x\\ \tilde{H}_y-\rho E_x\end{bmatrix}, \tag{6.1}$$

where ρ is a positive real number, we define the operator $\mathcal{B}'$ at any $z_*\geq z_0$, such that

$$\mathcal{B}'(z_*)\boldsymbol{v}'=-\boldsymbol{u}'\quad \text{at}\quad z=z_*, \tag{6.2}$$

for any electromagnetic field satisfying the Maxwell's equations (2.1) for $z<z_*$, a downward radiation condition (to be given below), and the quasi-periodic condition (2.8). For any nonzero electromagnetic field satisfying these conditions, we must have $\boldsymbol{v}'\neq\boldsymbol{0}$ at $z=z_*$. Otherwise, the z component of the time-averaged Poynting vector at z_* is

$$P_z=\frac{1}{2}\mathrm{Re}(E_x\overline{\tilde{H}}_y-E_y\overline{\tilde{H}}_x)=\frac{\rho}{2}(|E_x|^2+|\tilde{H}_x|^2)\geq 0. \tag{6.3}$$

The integral of P_z over one period in the $z=z_*$ plane is proportional to the power passing through one period in the positive z direction. Since the field satisfies a downward radiation condition and there is no source, the upward power should be zero, thus E_x and $\tilde{H}_x$ must be identically zero at z_*. The assumption $\boldsymbol{v}'=\boldsymbol{0}$ implies that E_y and $\tilde{H}_y$ must also vanish at z_*. This leads to the conclusion that all field components must be zero for $z\leq z_*$, since the Maxwell's equations can be written as a first order system for the x and y components, with only first order partial derivatives in z [20].

To march the operator $\mathcal{B}'$ through a layer, i.e., from z_{m-1} to z_m, we need the operator $\mathcal{M}^{(m)}$ satisfying

$$\mathcal{M}^{(m)}\begin{bmatrix}\boldsymbol{u}'(z_{m-1})\\ \boldsymbol{v}'(z_m)\end{bmatrix}=\begin{bmatrix}\mathcal{M}_{11}^{(m)} & \mathcal{M}_{12}^{(m)}\\ \mathcal{M}_{21}^{(m)} & \mathcal{M}_{22}^{(m)}\end{bmatrix}\begin{bmatrix}\boldsymbol{u}'(z_{m-1})\\ \boldsymbol{v}'(z_m)\end{bmatrix}=\begin{bmatrix}\boldsymbol{v}'(z_{m-1})\\ \boldsymbol{u}'(z_m)\end{bmatrix}. \tag{6.4}$$

Note the difference between this operator, where $\boldsymbol{u}'(z_{m-1})$ is in the left hand side, and $\mathcal{N}^{(m)}$ given in (3.5), where both $\boldsymbol{v}$ at z_m and z_{m-1} are in the left hand side. The operator $\mathcal{M}^{(m)}$ is well-defined for all frequencies, since a nonzero field cannot satisfy $\boldsymbol{u}'=\boldsymbol{0}$ at z_{m-1} and $\boldsymbol{v}'=\boldsymbol{0}$ at z_m, otherwise, it radiates power to $z<z_{m-1}$ and $z>z_m$. Notice that if $\boldsymbol{u}'=\boldsymbol{0}$, then $P_z=-\rho(|\tilde{H}_y|^2+|E_y|^2)/2\leq 0$. From the definitions of $\mathcal{B}'$ and $\mathcal{M}^{(m)}$, the following

marching formulae can be derived:

$$\mathcal{Z}=[\mathcal{I}+\mathcal{M}_{11}^{(m)}\mathcal{B}'(z_{m-1})]^{-1}\mathcal{M}_{12}^{(m)}, \tag{6.5}$$

$$\mathcal{B}'(z_m)=\mathcal{M}_{21}^{(m)}\mathcal{B}'(z_{m-1})\mathcal{Z}-\mathcal{M}_{22}^{(m)}. \tag{6.6}$$

For any $z_*\geq z_0$, we can define the operator $\mathcal{W}'$ by

$$\mathcal{W}'(z_*)\boldsymbol{v}'|_{z=z_*}=\boldsymbol{v}'|_{z=z_0}, \tag{6.7}$$

then the additional marching formula is

$$\mathcal{W}'(z_m)=\mathcal{W}'(z_{m-1})\mathcal{Z}. \tag{6.8}$$

Based on the vectors $\boldsymbol{u}'$ and $\boldsymbol{v}'$, we can establish a downward radiation condition valid for all frequencies. If $\boldsymbol{u}'$ and $\boldsymbol{v}'$ (for $z<0$) are expanded in plane waves with wave vectors $(\alpha_j,\beta_k,-\gamma_{jk}^{(2)})$, then their corresponding vector coefficients $\boldsymbol{a}_{jk}^{\prime(t)}$ and $\boldsymbol{b}_{jk}^{\prime(t)}$ are related to each other by

$$\boldsymbol{a}_{jk}^{\prime(t)}+B_{jk}^{\prime(t)}\boldsymbol{b}_{jk}^{\prime(t)}=0, \tag{6.9}$$

where

$$B_{jk}^{\prime(t)}=\frac{1}{\Delta_{jk}^{(2)}}\begin{bmatrix}\alpha_j\beta_k(1+\rho^2) & k_0\gamma_{jk}^{(2)}(\mu^{(2)}-\rho^2\varepsilon^{(2)})-\rho(\alpha_j^2-\beta_k^2)\\ k_0\gamma_{jk}^{(2)}(\rho^2\mu^{(2)}-\varepsilon^{(2)})+\rho(\alpha_j^2-\beta_k^2) & \alpha_j\beta_k(1+\rho^2)\end{bmatrix}, \tag{6.10}$$

and

$$\Delta_{jk}^{(2)}=\alpha_j^2+(\gamma_{jk}^{(2)})^2+\rho k_0\gamma_{jk}^{(2)}(\varepsilon^{(2)}+\mu^{(2)})+\rho^2[\beta_k^2+(\gamma_{jk}^{(2)})^2]. \tag{6.11}$$

Notice that $\Delta_{jk}^{(2)}\neq 0$ for all $k_0>0$. This allows us to define an operator $\mathcal{B}'^{(t)}$, so that the boundary condition at $z=0$, i.e., the downward radiation condition, can be written as

$$\boldsymbol{u}'+\mathcal{B}'^{(t)}\boldsymbol{v}'=\boldsymbol{0},\quad z=0. \tag{6.12}$$

The boundary condition at $z=D$ can be similarly derived, but it is necessary to use an operator that maps $\boldsymbol{u}'$ to $-\boldsymbol{v}'$. Expanding the reflected wave $\boldsymbol{u}'^{(r)}$ and $\boldsymbol{v}'^{(r)}$ for $z>D$ in plane waves, their vector coefficients corresponding to the wave vector $(\alpha_j,\beta_k,\gamma_{jk}^{(1)})$ are linked by the following 2×2 matrix

$$G_{jk}^{\prime(r)}=\frac{1}{\Delta_{jk}^{(1)}}\begin{bmatrix}\alpha_j\beta_k(1+\rho^2) & k_0\gamma_{jk}^{(1)}(\mu^{(1)}-\rho^2\varepsilon^{(1)})+\rho(\alpha_j^2-\beta_k^2)\\ k_0\gamma_{jk}^{(1)}(\rho^2\mu^{(1)}-\varepsilon^{(1)})-\rho(\alpha_j^2-\beta_k^2) & \alpha_j\beta_k(1+\rho^2)\end{bmatrix}, \tag{6.13}$$

where

$$\Delta_{jk}^{(1)}=\beta_k^2+(\gamma_{jk}^{(1)})^2+\rho k_0\gamma_{jk}^{(1)}(\varepsilon^{(1)}+\mu^{(1)})+\rho^2[\alpha_j^2+(\gamma_{jk}^{(1)})^2]. \tag{6.14}$$

This gives rise to an operator $\mathcal{G}'^{(r)}$ such that $\boldsymbol{v}'^{(r)}+\mathcal{G}'^{(r)}\boldsymbol{u}'^{(r)}=\mathbf{0}$ and the following boundary condition:

$$\boldsymbol{v}'+\mathcal{G}'^{(r)}\boldsymbol{u}'=[\boldsymbol{v}'^{(i)}+\mathcal{G}'^{(r)}\boldsymbol{u}'^{(i)}]_{z=D^+},\quad z=D. \tag{6.15}$$

At $z_0=0$, we can initialize the two operators $\mathcal{B}'$ and $\mathcal{W}'$ by

$$\mathcal{B}'(z_0)=\mathcal{B}'^{(t)},\quad \mathcal{W}'(z_0)=\mathcal{I}. \tag{6.16}$$

After $\mathcal{B}'$ and $\mathcal{W}'$ are obtained at $z_M=D$, we can solve $\boldsymbol{v}'(z_M)$ from

$$\Big[\mathcal{I}-\mathcal{G}'^{(r)}\mathcal{B}'(z_M)\Big]\boldsymbol{v}'(z_M)=[\boldsymbol{v}'^{(i)}+\mathcal{G}'^{(r)}\boldsymbol{u}'^{(i)}]_{z=D^+}, \tag{6.17}$$

then determine the reflected and transmitted waves.

While the above OM scheme avoids the difficulties associated with some special frequencies, its implementation becomes more complicated. Our view is that although the simpler OM scheme of Section 3 could fail in some cases, it is still useful, as far as we monitor the potential risk of failure. This can be done by avoiding the frequencies satisfying $k_0^2\varepsilon\mu=\alpha_j^2$ or $k_0^2\varepsilon\mu=\beta_k^2$ for integers j and k, and monitoring the norms of $\mathcal{B}$, $\mathcal{W}$, and $\mathcal{N}^{(m)}$. The numerical examples of the next section are based on the simple OM scheme of Section 3.

7 Numerical examples

In this section, we present numerical examples to validate and illustrate our method developed in previous sections. First, we consider 32 layers of crossed arrays of circular dielectric cylinders surrounded by air. As in previous works [18, 20], we assume that the cylinders have a dielectric constant $\varepsilon=5$ and a radius $0.25L$, where L is the period of the array in each layer and also the vertical distance between the cylinder centers in neighboring layers. More precisely, the layers are given by $z_{m-1}<z<z_m=z_{m-1}+L$ for $1\le m\le M=32$, the cylinders in the mth layer are parallel to the x axis if m is even and to the y axis if m is odd, and their axes are located on the plane at $z=(z_{m-1}+z_m)/2$. For a normal incident plane wave with the wavevector $(\alpha_0,\beta_0,-\gamma_{00}^{(1)})=(0,0,-k_0)$ and a magnetic field polarized in the y direction, we use our method to calculate the reflection spectra. The results shown in Fig. 2 are the reflection spectra for two cases, where R_{00} is the diffraction efficiency of the $(0,0)$-th reflection order, i.e., the normalized power carried by the $(0,0)$-th reflection order. The top panel is for regular crossed arrays where the centers of the cylinders in even (or odd) layers have the same x (or y) coordinates, or simply $x_c=y_c=0$ for all layers. The bottom panel is for a woodpile structure where x_c and y_c are alternatively 0 and $L/2$ in even and odd layers, respectively. Our results agree with those of [18] and are indistinguishable from those of [20]. For this example, we avoid the frequencies $\omega L/(2\pi c)=1/\sqrt{5}$ and $2/\sqrt{5}$ (assuming $\omega L/(2\pi c)<1$), since

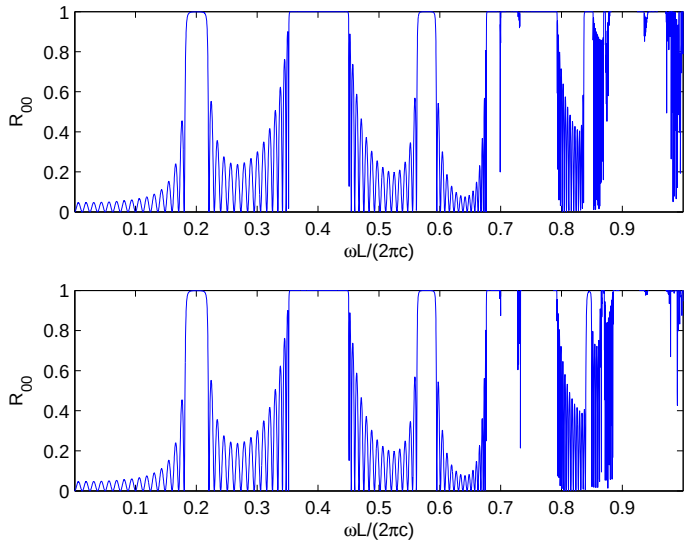

Figure 2: Reflection spectra for 32 layers of crossed arrays of circular cylinders. Top: regular arrays. Bottom: woodpile arrays.

formulae (5.3), (5.4), (5.12) and (5.13) (for constructing the field inside the rods) break down at these frequencies.

Next, we consider a dielectric slab with M crossed arrays of circular cylindrical air-holes. The dielectric constant of the slab is $\varepsilon=11.4$. The radius of the air-holes is $0.4L$, where L is the period in x and y directions. The cylindrical air-holes are arranged as a woodpile structure, where the axes of air-holes in two layers separated by one intermediate layer are offset by $L/2$. The thickness of the slab is $D=ML$. Assuming the slab is given by $0<z<D$, then the axes of the air-holes in the mth layer are located on the plane at $z=(m-0.5)L$. The medium above and below the slab (i.e. $z>D$ and $z<0$) is air. For this structure, we consider a plane incident wave with the wave vector $(0,0,-k_0)$ and an electric field polarized in the y direction. For $\omega L/(2\pi c)<1$ and the normal incident wave, the only propagating diffraction order is the $(0,0)$-th order. In Fig. 3, we show the transmission spectra for $M=8$ and $M=16$, where T_{00} is the diffraction efficiency of the $(0,0)$-th transmission order. These results are obtained with $N=N'=13$. For $\omega L/(2\pi c)\leq 0.5$, the OM scheme breaks down at $\omega L/(2\pi c)=1/\sqrt{11.4}$, and this frequency is avoided.

For the above air-hole structure, we also consider an oblique incident wave with a wave vector $(\alpha_0,\beta_0,-\gamma_{00}^{(1)})=k_0(\sqrt{6}/4,\sqrt{2}/4,-\sqrt{2}/2)$. For $M=16$, we show part of the transmission spectra in Fig. 4. The top and bottom panels correspond to incident waves with $\tilde{H}_y^{(i)}=0$ and $E_y^{(i)}=0$, respectively. At higher frequencies, there are more than one propagating transmission orders. In Fig. 5, we show the computed diffraction efficiencies of four transmission orders for different values of N (and $N'=N$). The left and right panels are results for $\omega L/(2\pi c)=0.9$ and $\omega L/(2\pi c)=1$, and for incident waves satisfying

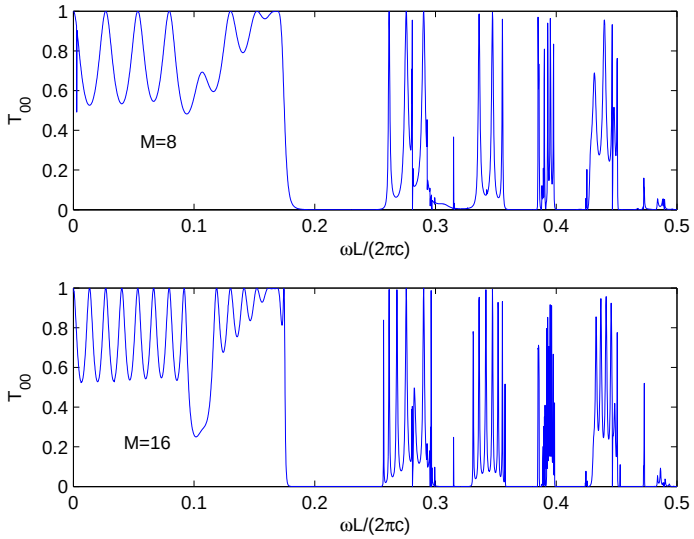

Figure 3: Transmission spectra of normal incident waves for woodpile crossed arrays of circular air-holes in a finite dielectric medium. Top: 8 layers. Bottom: 16 layers.

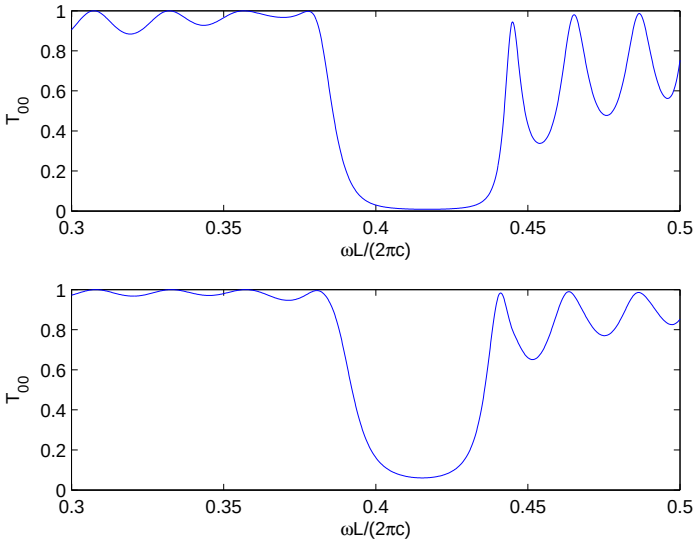

Figure 4: Transmission spectra of oblique incident waves for 16 layers of crossed arrays of air-holes in a dielectric medium. Top: $\tilde{H}_y^{(i)}=0$. Bottom: $E_y^{(i)}=0$.

$\tilde{H}_y^{(i)}=0$ and $E_y^{(i)}=0$, respectively. For practical applications, it is sufficient to use a very moderate value for N, such as $N=11$.

For this example and for frequencies satisfying $\omega L/(2\pi c)\leq 0.5$, we need to avoid

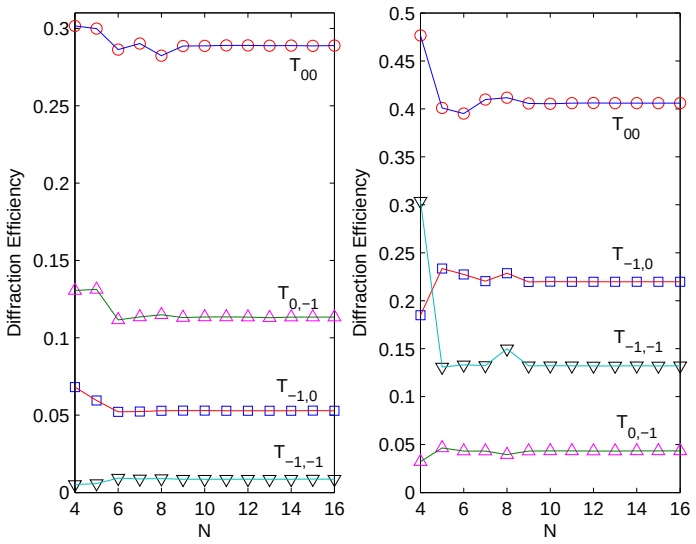

Figure 5: Dependence of diffraction efficiencies on integer N. Left: $\tilde{H}_y^{(i)}=0$ and $\omega L/(2\pi c)=0.9$. Right: $E_y^{(i)}=0$ and $\omega L/(2\pi c)=1$.

$\omega L/(2\pi c)=1/(\sqrt{11.4}\pm\sqrt{6}/4)$ and $1/(\sqrt{11.4}\pm\sqrt{2}/4)$, since the OM scheme breaks down at these frequencies. For frequencies near a breakdown value, we expect some loss of precision, but the effect appears to be very mild. For example, let ω_* be the frequency corresponding to $1/(\sqrt{11.4}+\sqrt{6}/4)$, we calculate T_{00} for $\omega=0.99\omega_*$, $0.999\omega_*$, $1.001\omega_*$ and $1.01\omega_*$, where the incident wave satisfies $\tilde{H}_y^{(i)}=0$. The results obtained using different values of N are listed the Table 1. In all cases, the first four digits are stabilized for N

Table 1: Transmission coefficient T_{00} of an oblique incident wave with $\tilde{H}_y^{(i)}=0$ for 16 layers of crossed arrays of air-holes in a dielectric medium. The frequencies are near the breakdown value $\omega_* L/(2\pi c)=1/(\sqrt{11.4}+\sqrt{6}/4)$.

N	$T_{00}(0.99\omega_*)$	$T_{00}(0.999\omega_*)$	$T_{00}(1.001\omega_*)$	$T_{00}(1.01\omega_*)$
6	0.8747	0.8051	0.7947	0.7751
7	0.8765	0.8074	0.7972	0.7785
8	0.8748	0.8059	0.7958	0.7776
9	0.8745	0.8054	0.7953	0.7768
10	0.8749	0.8058	0.7956	0.7771
11	0.8750	0.8059	0.7957	0.7772
12	0.8749	0.8058	0.7956	0.7772
13	0.8749	0.8058	0.7956	0.7771
14	0.8749	0.8058	0.7956	0.7771
15	0.8749	0.8058	0.7956	0.7771

around 12 or 13. In our implementation, the norms of $\mathcal{B}$, $\mathcal{W}$ and $\mathcal{N}^{(m)}$ are continuously monitored, so that any possible loss of precision can be automatically detected.

8 Conclusions

In this paper, we develop a new semi-analytic method (called T2T operator marching method) to analyze transmission and reflection properties for structures with crossed arrays of circular cylinders. The method marches two operators $\mathcal{B}$ and $\mathcal{W}$ through the structure layer-by-layer, where each layer is an infinite periodic array of circular cylinders parallel to the x or y axis, using local operators $\mathcal{N}^{(m)}$ constructed from cylindrical wave expansions. The construction of $\mathcal{N}^{(m)}$ is efficient, since it is reduced to a sequence of 2D problems which have analytic solutions. The operator $\mathcal{B}$ and $\mathcal{N}^{(m)}$ are named global and local T2T operators, respectively, since they map tangential field components in one spatial direction to tangential field components in another spatial direction. Compared with the earlier method developed in [20], the new method brings a number of simplifications. Since $\mathcal{B}$ and $\mathcal{W}$ are continuous, there is no need for steps to jump over horizontal interfaces. Furthermore, the same local operator $\mathcal{N}^{(m)}$ is used in the marching process whether the cylinders in a layer are parallel to the x or y axis, therefore, it is not necessary to use two pairs of operators and to switch between them. The method is validated by comparing numerical solutions with those given in [18] and [20]. It is further illustrated by a slab structure where the cylinders are actually air-holes in the slab.

The operator marching procedure makes the method particularly efficient for structures with many layers. The method is useful to design structures with crossed arrays for practical applications. The main operator-marching step is valid even when the cylinders in the layers have general cross sections, but a different method must be used to construct the local T2T operators $\mathcal{N}^{(m)}$.

The relatively simple OM scheme developed in Sections 3, 4 and 5 could break down at some special frequencies. A more robust OM scheme is proposed in Section 6. However, the simple scheme is still useful, since we can detect any significant loss of accuracy by monitoring the norms of $\mathcal{B}$, $\mathcal{W}$ and $\mathcal{N}^{(m)}$. In our experience, the method remains reliable even when the frequency only differs from a breakdown point by 0.1% in relative values. Finally, it is clearly worthwhile to implement the more robust OM scheme of Section 6 and to develop OM schemes for more general 3D periodic structures.

Acknowledgments

This work was partially supported by Fudan University under The Talent Recruitment Grant No. IDH1207001, and by the Research Grants Council of Hong Kong Special Administrative Region, China, under Project CityU 102411.

References

[1] R. Petit, Electromagnetic Theory of Gratings, Springer-Verlag, 1980.
[2] G. Bao, L. Cowsar and W. Masters, Mathematical Modeling in Optical Science, Society for Industrial and Applied Mathematics, Philadelphia, 2001.
[3] M. Nevière and E. Popov, Light Propagation in Periodic Media, Marcel Dekker, Inc. 2003.
[4] J. D. Joannopoulos, S. G. Johnson, J. N. Winn, and R. D. Meade, Photonic Crystals: Molding the Flow of Light, 2nd ed., Princeton Uiversity Press, 2008.
[5] W. Cai and V. Shalaev, Optical Metamaterials: Fundamentals and Applications, Springer, 2010.
[6] K. M. Ho, C. T. Chan, C. M. Soukoulis, R. Biswas, and M. Sigalas, Photonic band gaps in three dimensions: New layer-by-layer periodic structures, Solid State Communications, 89 (1994), 413-416.
[7] H. S. Sözüer and J. P. Dowling, Photonic band calculations for woodpile structures, J. Mod. Opt., 41 (1994), 231-239.
[8] D. Zhao, H. Yang, Z. Ma, and W. Zhou, Polarization independent broadband reflectors based on cross-stacked gratings, Opt. Express, 19 (2011), 9050-9055.
[9] D. C. Dobson and A. Friedman, The time harmonic Maxwell equations in a doubly periodic structure, J. Math. Anal. Appl., 166 (1992), 507-528.
[10] D. C. Dobson, A variational method for electromagnetic diffraction in biperiodic structures, Modél. Math. Anal. Numér., 28 (1994), 419-439.
[11] G. Bao, A variational approximation of maxwell's equations in biperiodic structures, SIAM J. Appl. Math., 57 (1997), 364-381.
[12] G. Bao and D. C. Dobson, On the scattering by a biperiodic structure, Proc. AMS, 128 (2000), 2715-2723.
[13] J. M. Jin, The Finite Element Method in Electromagnetics, 2nd ed., John Wiley & Sons, 2002.
[14] P. Monk, Finite Element Methods for Maxwell's Equations, Clarendon Press, Oxford, 2003.
[15] G. Bao, Z. M. Chen, and H. J. Wu, Adaptive finite-element method for diffraction gratings, J. Opt. Soc. Am. A, 22 (2005), 1106-1114.
[16] G. Bao, P. Li, and H. J. Wu, An adaptive edge element method with perfectly matched absorbing layers for wave scattering by biperiodic structures, Mathematics of Computation, 79 (2010), 1-34.
[17] G. H. Smith, L. C. Botten, R. C. McPhedran, and N. A. Nicorovici, Cylinder gratings in conical incidence with applications to woodpile structures, Phys. Rev. E, 67 (2003), 056620. (2003).
[18] K. Yasumoto and H. Jia, Electromagnetic scattering from multilayered crossed-arrays of circular cylinders, Proceedings of SPIE, 5445 (2004), 200-205.
[19] J. M. Borwein, M. L. Glasser, R. C. McPhedran, J. G. Wan, and I. J. Zucker, Lattice Sums Then and Now, Cambridge University Press, 2013.
[20] Y. Wu and Y. Y. Lu, Dirichlet-to-Neumann map method for analyzing crossed arrays of circular cylinders, J. Opt. Soc. Am. B, 26 (2009), 1984-1993.
[21] D. Maystre, A new general integral equation theory for dielectric coated gratings, J. Opt. Soc. Am., 68 (1978), 490-495.
[22] D. Maystre, Electromagnetic study of photonic band gaps, Pure Appl. Opt., 3 (1994), 975-993.
[23] L. Li, Formulation and comparison of two recursive matrix algorithms for modeling layered diffraction gratings, J. Opt. Soc. Am. A, 13 (1996), 1024-1035.
[24] Y. Y. Lu and J. R. McLaughlin, The Riccati method for the Helmholtz equation, J. Acoust.

Soc. Am., 100 (1996), 1432-1446.
[25] Y. Y. Lu, Some techniques for computing wave propagation in optical waveguides, Communications in Computational Physics, 1 (2006), 1056-1075.
[26] Z. Hu and Y. Y. Lu, Improved Dirichlet-to-Neumann map method for modeling extended photonic crystal devices, Optical and Quantum Electronics, 40 (2008), 921-932.
[27] L. Goray and G. Schmidt, Analysis of two-dimensional photonic band gaps of any rod shape and conductivity using a conical-integral-equation method, Phys. Rev. E, 85 (2012), 036701.
[28] G. Schmidt, Conical diffraction by multilayer gratings: A recursive integral equation approach, Applications of Mathematics, 58 (2013), 279-307.
[29] Y. Wu and Y. Y. Lu, Dirichlet-to-Neumann map method for analyzing periodic arrays of cylinders with oblique incident waves, J. Opt. Soc. Am. B, 26 (2009), 1442-1449.
[30] M. J. Gander, F. Magoulès, and F. Nataf, Optimized Schwarz methods without overlap for the Helmholtz equation, SIAM J. Sci. Comput., 24 (2002), 38-60.
[31] M. Ehrhardt, J. Sun, and C. Zheng, Evaluation of scattering operator for semi-infinite periodic arrays, Commun. Math. Sci., 7 (2009), 347-364.